Available online at www.sciencedirect.com
SCIENCE DIRECT®
Journal of Chromatography A, 1041 (2004) 77–85
JOURNAL OF CHROMATOGRAPHY A
www.elsevier.com/locate/chroma

Modeling chromatographic columns Non-equilibrium packed-bed adsorption with non-linear adsorption isotherms

Ahmet R. Özdural [a,*], Aslı Alkan [a], Piet J.A.M. Kerkhof [b]

[a] *Department of Chemical Engineering, Hacettepe University, Beytepe, 06532 Ankara, Turkey*
[b] *Department of Chemical Engineering and Chemistry, Eindhoven University of Technology, P.O. Box 513, 5600 MB, Eindhoven, The Netherlands*

Received 1 October 2003; received in revised form 23 February 2004; accepted 6 May 2004

Abstract

In this work a new mathematical model, based on non-equilibrium conditions, describing the dynamic adsorption of proteins in columns packed with spherical adsorbent particles is used to study the performance of chromatographic systems. Simulations of frontal chromatography, including axial dispersion, for non-equilibrium systems with non-linear adsorption isotherms are made and compared to those of the experimentally determined protein A affinity chromatography breakthrough curves of *h*IgG, gathered from the literature. The non-equilibrium model developed here combines external mass transfer and intra-particle transport by solid (surface) diffusion, and permits the prediction of (time and bed height dependent) interface and average solid concentrations, along with interface and bulk liquid concentrations. The present non-equilibrium approach significantly improved the model predictions of experimentally observed distended breakthrough fronts over local equilibrium based models, and can be used to evaluate the influence of system parameters on the performance of chromatographic packed-bed adsorption columns.

Keywords: Mathematical modelling; Adsorption; Numerical analysis; Surface diffusion; Protein A; Proteins

1. Introduction

Frontal chromatography is a widely used process in the purification of biopharmaceuticals. Simulations of chromatographic processes are useful for studying and understanding complex column dynamics. In packed-bed adsorption, the complexity of the problem increases if the usually assumed condition of local equilibrium is not invoked. The local equilibrium model neglects all transient resistances, i.e. there is no concentration gradient within a particle or in the liquid film. Local equilibrium assumption between fluid and solid phases is assumed by many authors, thus greatly simplifying their equations [1–10]. For the cases of realistic mass transfer resistances, and especially for non-linear adsorption isotherms, local equilibrium based models usually become less effective in predicting experimentally observed distended breakthrough fronts and causes the predicted curves to be too sharp [11–13].

Yao and Tien [14] showed that, for systems with linear adsorption isotherms, the classic LDF expression is equivalent to the solution of the intraparticle diffusion equation and extended their analysis [15] to systems with non-linear adsorption isotherms. For the case of surface diffusion model they concluded that, due to the approximate solution, the error introduced was of the order of $[c(x,t) - c_s^*(x,t)]^2$ where $c_s^*(x,t)$ is the interphase liquid concentration (mg/cm^3) adjacent to the adsorbent surface which is in equilibrium with $q_s(x,t)$, and $c(x,t)$ is the bulk liquid concentration (mg/cm^3) in the void fraction of packed-bed adsorption column, as shown in Fig. 1. This leads to the conclusion that the solution of Yao and Tien [15] becomes free from errors if $c(x,t) \cong c_s^*(x,t)$. Such a case is of course only possible when local equilibrium assumption holds. Fig. 1 schematically represents the solute adsorption in a spherical homogeneous adsorbent particle which is free from the local equilibrium assumption between solid average concentration, $\bar{q}(x,t)$ and

* Corresponding author. Fax: +90-312-299-2124.
E-mail address: ozdural@hacettepe.edu.tr (A.R. Özdural).

0021-9673/$ – see front matter © 2004 Elsevier B.V. All rights reserved.
doi:10.1016/j.chroma.2004.05.009

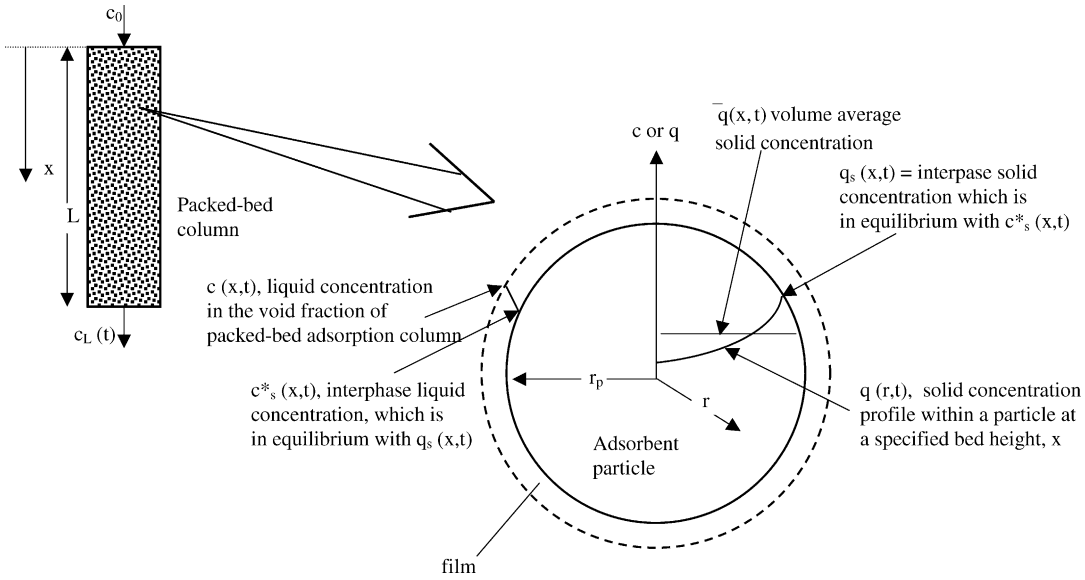

Fig. 1. Solute adsorption in a spherical adsorbent particle.

bulk liquid concentration, $c(x, t)$ due to the fact that equilibrium is not attained instantaneously but follows a given kinetics. The film concentration gradient might only be flattened at near saturation conditions and thus local equilibrium assumption might become valid. Otherwise, since adsorption itself is generally very fast, it is reasonable to state that equilibrium is attained at the interface ie. adsorbent phase surface concentration, $q_S(x, t)$ reaches to the equilibrium with the surface of the liquid film that is next to the adsorbent, $c_S^*(x, t)$. Therefore, throughout the adsorption process, until near saturation, non-equilibrium conditions prevail.

Lumped rate models, where overall mass transfer coefficients have been used by combining the film and particle mass transfer resistances, took the interest of researchers [11,16–21]. For linear systems, pore diffusion lumped models can fit the breakthrough curves well but might give inaccurate pore diffusion coefficients [22]. Another approach [23,24] for non-equilibrium adsorption modeling is to envisage an instant equilibrium between bulk fluid concentration and solid surface concentration, as an alternative to the local equilibrium (instant equilibrium between bulk fluid concentration and solid average concentration) assumption. However, such an approach leads to intraparticle resistance controlling, and neglects external film resistance.

Resistance to mass transfer in adsorption processes is usually based on a dual resistance model combining external mass transfer and intraparticle transport. The major differences in the models are due to the mechanism of intraparticle diffusion proposed, namely pore diffusion, surface (solid) diffusion or a combination of both. Pore diffusion model assumes that the adsorbate diffuses in the pores of the adsorbent, and is adsorbed on the surface of the pores. An additional assumption is that the adsorption rate is much faster than the diffusion rate [25–27]. Choy et al. [28] have studied batch adsorption with a two-resistance model based on external mass transfer and pore diffusion by incorporating a time dependent hypothetical equilibrium solid phase concentration. They assumed that there is an unreacted core, shrinking in size as adsorption proceeds. The surface (solid) diffusion model considers the intraparticle resistance in the form of surface (solid) diffusion and has been successfully employed for characterizing mass transfer processes associated with the adsorption of solutes onto adsorbents or ion exchange adsorbents [25,26,29–33].

In this work, a new and efficient mathematical model describing the dynamic adsorption of proteins in columns packed with spherical adsorbent particles is used to study the performance of chromatographic systems operating under non-equilibrium conditions with non-linear adsorption isotherms. Several groups of researchers have proposed and solved packed-bed adsorption models using different numerical approaches [34–36]. These models are generally based on a “coupled” partial differential equation (PDE) system with two sets of mass balance equations in the bulk fluid and particle phases, and thus require the use of advanced numerical methods such as orthogonal collocation or finite element so as to save memory space with reasonable efficiency and accuracy. The present approach obviates the solution of “coupled” PDE systems, and employs a single set of PDE by crediting the present time particle phase concentration at a specified bed location (situated between the two consecutive panels) through the use of one time step prior to the present time particle phase concentration, and the bulk fluid inlet and outlet concentration differences, which concurrently takes into account the accumulation and axial dispersion effects.

Simulations of frontal chromatography, including axial dispersion, were made and compared to those of the experimentally determined protein A affinity chromatography breakthrough curves of *h*IgG, gathered from the literature

[10]. The present non-equilibrium approach significantly improved the model predictions of experimentally observed distended breakthrough fronts over local equilibrium based models, and can be used to evaluate the influence of system parameters on the performance of chromatographic packed-bed adsorption columns.

It is sought in this paper to accomplish the following with the introduction of a new non-equilibrium model which is free from the limitations of the above mentioned non-equilibrium models: (1) to demonstrate the effect of the feed inlet concentration on the time and bed height dependent interface and bulk liquid concentrations; (2) to show the dynamic behavior of solid phase average concentrations and solid phase surface concentrations and thus to suggest protocols for new system operations and/or scale-up processes of chromatographic packed-bed adsorption columns.

2. Theoretical

The mathematical model used in this work considers that single component adsorption takes place from a flowing liquid stream in a packed-bed chromatographic column (inside radius = R_c cm, bed height = L cm, bed void fraction = ε) of spherical adsorbent particles (radius = r_p cm) under isothermal conditions. The change of interstitial velocity of the liquid stream, v (cm/s), and the liquid concentration gradients in the radial direction of the bed are considered to be negligible. A constant surface (solid) diffusivity, D_s (cm^2/s) is used. Non-equilibrium conditions exist between the adsorbent particle and the liquid in the void fraction of packed-bed chromatographic adsorption column. It is assumed that the non-linear equilibrium data can be represented by Langmuir equation. The model is based on a dual resistance model combining external mass transfer and intraparticle transport by solid (surface) diffusion, and assumes a parabolic concentration profile within the particle. Eq. (1) shows the mathematical expression of the parabolic concentration profile.

$$\bar{q}(x,t) = a(x,t) + b(x,t)r^2 \tag{1}$$

where $\bar{q}(x,t)$ is the time and bed height dependent average solid concentration (mg/cm^3 solid, including particle pores volume) and $a(x,t)$ and $b(x,t)$ are the coefficients. Gleuckauf and Coates [37] proposed the linear driving force (LDF) model and they described that the adsorption rate of a single adsorbate into an adsorbent particle is essentially proportional to the amount of adsorbate still required to produce equilibrium in the adsorbent. Yao and Tien [14] derived the batch adsorption version of Eq. (2), by using the LDF approximation. Goto et al. [38] and Tejeda-Mansir et al. [39] showed that the LDF approximation is equivalent to the parabolic concentration profile assumption within the particle.

$$q_s(x,t) = \bar{q}(x,t) + \frac{Bi}{5}[c(x,t) - c_s^*(x,t)] \tag{2}$$

where Bi is the Biot number ($k_f r_p/D_s$). Eq. (3) gives the Langmuir adsorption isotherm expression [40]. Due to the realistic mass transfer resistances, i.e. non-equilibrium conditions as shown in Fig. 1, the widely used instant equilibrium (local equilibrium assumption) between the solid average concentration, $\bar{q}(x,t)$ and the bulk liquid concentration $c(x,t)$ is ruled out under dynamic conditions. However, it is reasonable to assume that $c_s^*(x,t)$ is in equilibrium with $q_s(x,t)$ since adsorption itself (transfer of solute at the interphase to adsorbed state) is generally very fast.

$$q_s(x,t) = \frac{q_m K_L c_s^*(x,t)}{1 + K_L c_s^*(x,t)} \tag{3}$$

From Eqs (2) and (3), we obtain the following relationship:

$$[c_s^*(x,t)]^2 + \left[\frac{5q_m}{Bi} - \frac{5\bar{q}(x,t)}{Bi} + \frac{1}{K_L} - c(x,t)\right] c_s^*(x,t) - \frac{1}{K_L}\left[c(x,t) + \frac{5\bar{q}(x,t)}{Bi}\right] = 0 \tag{4}$$

The positive root of Eq. (4) is

$$c_s^*(x,t) = \frac{-M + \sqrt{M^2 + 4/K_L[c(x,t) + 5\bar{q}(x,t)/Bi]}}{2} \tag{5}$$

where

$$M = \frac{5q_m}{Bi} - \frac{5\bar{q}(x,t)}{Bi} + \frac{1}{K_L} - c(x,t) \tag{6}$$

A differential mass balance gives the well known governing equation for a packed-bed adsorption column [41].

$$\frac{\partial c(x,t)}{\partial t} + v\frac{\partial c(x,t)}{\partial x} + \beta[c(x,t) - c_s^*(x,t)] = D_a\frac{\partial^2[c(x,t)]}{\partial x^2} \tag{7}$$

where

$$\beta = \frac{3(1-\varepsilon)}{\varepsilon r_p}k_f \tag{8}$$

Regarding the mass transfer resistances, Eq. (7) contains the k_f term only, but as shown in Eq. (2) surface diffusivity is inherently included in $c_s^*(x,t)$ term. Furthermore, there are two dependent variables, $c(x,t)$ and $c_s^*(x,t)$ and two independent variables, x and t. Substitution of Eq. (5) into Eq. (7) gives:

$$\frac{\partial[c(x,t)]}{\partial t} + v\frac{\partial[c(x,t)]}{\partial x} + \beta\left[c(x,t) - \frac{\sqrt{M^2 + 4/K_L[c(x,t) + 5\bar{q}(x,t)/Bi]} - M}{2}\right] = D_a\frac{\partial^2[c(x,t)]}{\partial x^2} \tag{9}$$

Under non-linear conditions such as the present case, there are no analytical solutions for Eq. (9). Solutions must be

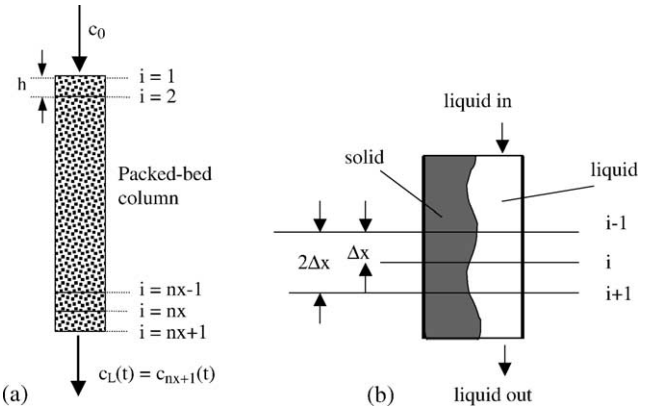

Fig. 2. Schematic representation of a packed-bed adsorption column for mathematical analysis: (a) general display, (b) display for the calculation of solid average concentrations.

calculated numerically with the following initial and boundary conditions. Furthermore, solution of Eq. (9) requires the use of average concentration in the adsorbent, $\bar{q}(x,t)$ value, which is addressed after the presentation of the liquid side equations.

I.C.	$t = 0$	for all x in the packed-bed	$c(x,t) = 0$
B.C. 1	for $t > 0$	$x = 0$	$c(x,t) = c_0$
B.C. 2	for $t > 0$	$x = L$	$\partial[c(x,t)]/\partial x = 0$

The second boundary condition is defined by the stop of mass transfer at the column outlet, where c_0 (mg/cm^3) is the constant liquid inlet concentration. In the present work the finite difference technique has been employed to provide a numerical solution. Since explicit schemes may suffer from stability limits the implicit scheme is used, where $\partial[c(x,t)]/\partial x$ and $\partial^2[c(x,t)]/\partial x^2$ are evaluated by the central difference approximation and $\partial[c(x,t)]/\partial t$ is evaluated by the backward difference approximation. Fig. 2a shows the schematic representation of a packed-bed chromatographic adsorption column for numerical analysis. The column is divided into n hypothetical slices of thickness $\Delta x = h$, where the time increment was $\Delta t = k$. For distance, x and time, t step indices of i and j are used, respectively. Instead of applying above given B.C. at $x = L$, we approximated the $c(x,t)|_{x=L}$ values at $i = nx + 1$ by linear extrapolation of $c(x,t)$ values at $i = nx - 1$ and $i = nx$.

$$\begin{aligned} &i = 1 \text{ (packed- inlet)} \\ &c_{i,j+1} = c_{i,j} = c_0 \\ &1 < i < nx + 1 \end{aligned} \tag{10}$$

Evaluating $\partial[c(x,t)]/\partial x$ and $\partial^2[c(x,t)]/\partial x^2$ by the central difference approximation, and $\partial[c(x,t)]/\partial t$ by the backward difference approximation [42] and substituting them into Eq. (9) gives

$$-(\alpha+\gamma)c_{i-1,j+1} + (1+2\gamma)c_{i,j+1} + (\alpha-\gamma)c_{i+1,j+1} = (1-\beta k)c_{i,j} + \frac{\beta k}{2}\left[\sqrt{M^2 + \frac{4}{K_L}\left(c_{i,j} + \frac{5\bar{q}_{i,j}}{Bi}\right)} - M\right] \tag{11}$$

where

$$\alpha = \frac{kv}{2h} \tag{12}$$

$$\gamma = \frac{kD_a}{h^2} \tag{13}$$

Eq. (11) requires the use of the average adsorbate concentration of adsorbent, $\bar{q}_{i,j}$ value. Let us consider Fig. 2b, where imaginarily adsorbent (solid) and liquid are accumulated on opposite sides of the column. During the time step $\Delta t = k$, material balance for panels between $i-1$ and $i+1$ gives $\bar{q}_{i,j}$ value for panel i, where $\Delta x = h$.

$$\bar{q}_{i,j} = \bar{q}_{i,j-1} + \frac{\varepsilon k}{2(1-\varepsilon)h}\left[v(c_{i-1,j} - c_{i+1,j}) - 2h\frac{\partial c(x,t)}{\partial t} + \frac{D_a(c_{i-1,j} - 2c_{j,i} + c_{i+1,j})}{h}\right] \tag{14}$$

The value of $\partial c(x,t)/\partial t$ term, shown in Eq. (14) can be expressed with finite difference equations. In order to find $\bar{q}_{i,j}$, let us express $\partial c(x,t)/\partial t$ again with a backward difference approximation, but in this case one time step earlier then that of the backward difference approximation of $\partial c(x,t)/\partial t$. Hence, for the calculation of c values at $j+1$ time, the $\bar{q}$ values at j time shall be employed in Eq. (11).

$$\frac{\partial c(x,t)}{\partial t} = \frac{-c_{i,j-1} + c_{i,j}}{k} \tag{15}$$

Substitution of Eq. (15) into Eq. (14) gives

$$\bar{q}_{i,j} = \bar{q}_{i,j-1} + \alpha\frac{\varepsilon}{1-\varepsilon}(c_{i-1,j} - c_{i+1,j}) - \frac{\varepsilon}{1-\varepsilon}(c_{i,j} - c_{i,j-1}) + \gamma\frac{\varepsilon}{1-\varepsilon}(c_{i-1,j} - 2c_{i,j} + c_{i+1,j}) \tag{16}$$

$i = nx + 1$ (packed-bed outlet).

It is assumed that the liquid concentration at $i = nx + 1$ can be calculated by extrapolating $i = nx - 1$ and $i = nx$ data.

$$c_{nx-1,j+1} - 2c_{nx,j+1} + c_{nx+1,j+1} = 0 \tag{17}$$

The left-hand side of Eq. (10) is known and it is equal to the constant liquid inlet concentration. The variables on the left-hand side of Eqs. (11) and (17) are unknown. However, if we have a grid of $n+1$ spatial points, then at time $j+1$ there are $n+1$ unknown nodal values. We can assemble the set of $n+1$ equations of the form given in Fig. 3. By solving the equation system presented in Fig. 3, we determine

$$\begin{bmatrix} 1 & 0 & 0 & 0 & \dots & \dots & 0 & 0 & 0 \\ -(\alpha+\gamma) & 1+2\gamma & \alpha-\gamma & 0 & 0 & \dots & \dots & 0 & 0 \\ 0 & -(\alpha+\gamma) & 1+2\gamma & \alpha-\gamma & 0 & \dots & \dots & \dots & 0 \\ 0 & 0 & -(\alpha+\gamma) & 1+2\gamma & \alpha-\gamma & 0 & \dots & \dots & 0 \\ \dots & \dots & \dots & \dots & \dots & \dots & \dots & \dots & \dots \\ \dots & \dots & \dots & 0 & -(\alpha+\gamma) & 1+2\gamma & \alpha-\gamma & 0 & \dots \\ 0 & \dots & \dots & \dots & 0 & -(\alpha+\gamma) & 1+2\gamma & \alpha-\gamma & 0 \\ 0 & \dots & \dots & \dots & \dots & 0 & -(\alpha+\gamma) & 1+2\gamma & \alpha-\gamma \\ 0 & 0 & \dots & \dots & \dots & 0 & 1 & -2 & 1 \end{bmatrix} \mathbf{x} \begin{bmatrix} c_{1,j+1} \\ c_{2,j+1} \\ c_{3,j+1} \\ \dots \\ \dots \\ \dots \\ c_{nx-1,j+1} \\ c_{nj+1} \\ c_{nx+1,j+1} \end{bmatrix} = \begin{bmatrix} c_0 \\ (1-\beta k)c_{2,j} + \frac{\beta k}{2}\left[\sqrt{M^2 + \frac{4}{K_L}(c_{2,j} + \frac{5\bar{q}_{2,j}}{Bi})} - M\right] \\ (1-\beta k)c_{3,j} + \frac{\beta k}{2}\left[\sqrt{M^2 + \frac{4}{K_L}(c_{3,j} + \frac{5\bar{q}_{3,j}}{Bi})} - M\right] \\ \dots \\ \dots \\ \dots \\ \dots \\ (1-\beta k)c_{nx,j} + \frac{\beta k}{2}\left[\sqrt{M^2 + \frac{4}{K_L}(c_{nx,j} + \frac{5\bar{q}_{nx,j}}{Bi})} - M\right] \\ 0 \end{bmatrix}$$

Fig. 3. Assembly of the set of $n+1$ equations for numerical solution.

$c_1, c_2, \dots, c_{n+1}$ at time step $j+1$ from $c_1, c_2, \dots, c_{n+1}$ at time step j. Özdural et al. [43,44] employed a similar solution methodology to packed-bed enzyme reactors and to flat plate dialyzers [45].

3. Simulation results and comparison with the experimental data

The validity of the non-equilibrium model predictions were checked by comparing the simulated results with experimental data from literature. McCue et al. [10] used two different pore sizes of protein-A chromatography media (PG 700 and PG 1000, obtained from Millipore, Bedford, MA, USA). The authors concluded that the Langmuir model successfully represents the experimental adsorption isotherms, and performed frontal chromatography studies, by loading solution of *h*IgG in PBS (1 mg/cm^3) onto the columns under two different (250 and 500 cm/h) superficial velocities, where free solution diffusivity of *h*IgG was calculated as 4.0×10^{-7} cm^2/s. Experimental and local equilibrium based models predicted breakthrough profiles of *h*IgG on PG 700 and PG 1000 were presented as Figs. 4 and 5 in their article. The authors kindly provided the experimental data upon our request [46]. The system and operating parameters are summarized in Table 1. Prior to the non-equilibrium simulation studies, film mass transfer and axial dispersion coefficients are calculated for the system of interest and given in Table 2. Since the feed at the column inlet is a dilute solution, for solution density and viscosity, properties of pure water are used.

The well-known correlation of Wilson and Geankoplis [47] for mass transfer of liquids in packed-beds was used

Table 1
Chromatography media (porous glass, PG 700 and PG 1000) and column properties to be used in the prediction of breakthrough profiles of *h*IgG. Data from McCue et al. [10]

Properties	PG 700	PG 1000
Bulk density (g/cm^3)	0.39	0.38
Particle porosity (–)	0.68	0.69
Average particle diameter (μm)	100	100
Bed voidage (–)	0.43	0.45
Bed height (cm)	20.0	6.0
Column i.d. (cm)	0.66	0.66
Langmuir isotherm q_m value (mg/cm^3 media)	121	76
Langmuir isotherm K_L value (cm^3/mg)	18.9	13.1

Table 2
Axial dispersion, D_a and film mass transfer, k_f coefficients calculated through Eqs. (18) and (19)

u (cm/h)	PG 700[a]		PG 1000[a]	
	20 cm[b]		6 cm[b]	
	$k_f \times 10^3$ (cm/s)	$D_a \times 10^3$ (cm^2/s)	$k_f \times 10^3$ (cm/s)	$D_a \times 10^3$ (cm^2/s)
250	1.22	3.27	1.16	3.58
500	1.54	6.50	1.47	7.12

[a] Media.
[b] Bed height.

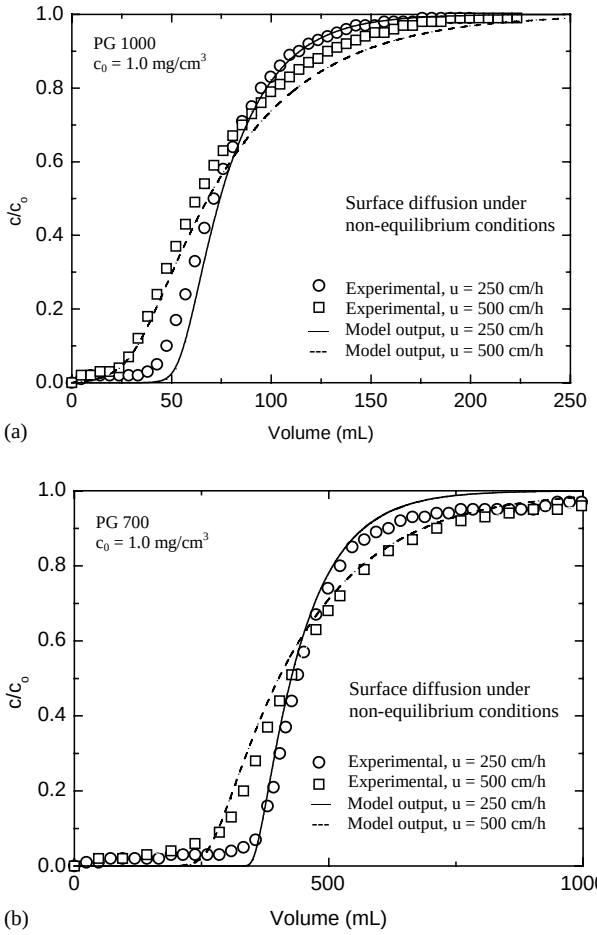

Fig. 4. Experimental and the proposed homogeneous surface diffusion under non-equilibrium conditions model predicted breakthrough profiles of hIgG on: (a) PG 1000 chromatography media, (b) PG 700 chromatography media. *Note*: Experimental data of Figs. 4 and 5 of McCue et al. [10] are kindly supplied by the authors, with permission from Elsevier, Copyright (2003).

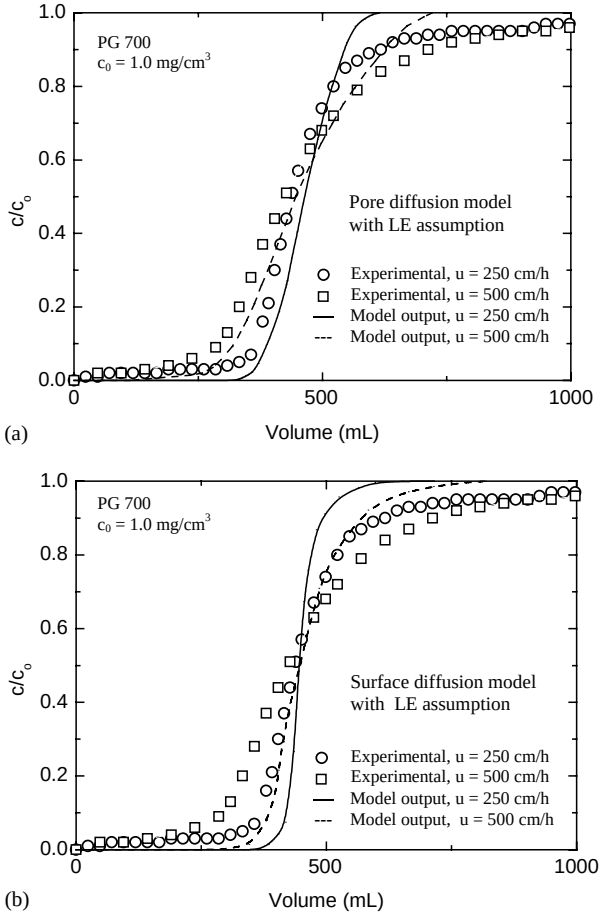

Fig. 5. Experimental and (a) pore diffusion, (b) homogeneous surface diffusion model (LE assumption) predicted breakthrough profiles of *h*IgG on PG 700 chromatography media. *Note*: Experimental data of Fig. 4 of McCue et al. [10] are kindly supplied by the authors, with permission from Elsevier, Copyright (2003).

for evaluating the film mass transfer coefficient, where Sherwood number ($Sh = 2r_p k_f/D$) is expressed in terms of Reynolds ($Re = 2r_p u\rho/\mu$) and Schmidt number ($Sc = \mu/\rho D$).

$$Sh = \left(\frac{1.09}{\varepsilon}\right) Re^{1/3}\, Sc^{1/3} \tag{18}$$

for $0.0016 < Re < 55$ and $165 < Sc < 70600$.

The axial dispersion coefficient, D_a for liquids in packed beds has been studied by several researchers. Their results have been collected and presented graphically [48,49]. D_a values for the present conditions are calculated using the following empirical Peclet number ($Pe = 2r_p v/D_a$) versus Reynolds number correlation [50]. This relation is based on numerous experiments over a broad range of *Re* numbers (10^{-3} to 10^3).

$$\varepsilon Pe = 0.20 + 0.011\, Re^{0.48} \tag{19}$$

We have determined the bed height dependent bulk liquid concentration, *c* and the liquid film interphase concentration, c_s^* versus accumulated volume (that represents time) profiles, through homogeneous surface diffusion under non-equilibrium conditions model proposed in this study, for the parameter values given in Tables 1 and 2. We have also determined the corresponding profiles of adsorbent particle average concentration, $\overline{q}$ and adsorbent particle surface concentration, q_s. Fig. 4 gives the experimentally determined breakthrough profiles of McCue et al. [10] for columns packed with: (a) PG 1000, (b) PG 700 chromatography media, along with the non-equilibrium model breakthrough curve predictions of the present study. The authors [10] used a long bed (20 cm) for PG 700 and a short bed for PG 1000 (6 cm) with a constant column inside diameter (i.d. = 0.66 cm), and employed two different liquid superficial velocities ($u = 250$ and 500 cm/h) with an inlet concentration of 1.0 mg/cm^3. During the model calculations we used D_s values of 0.48×10^{-9} and 1.8×10^{-9} cm^2/s for PG 700 and PG 1000, respectively. These values are consistent with those of McCue et al. [10] where they obtained a series of D_s values for different initial tank concentrations from the fitting of stirred tank experimental uptake

data. The chromatographic media content of their column studies increases with the bed length and thus during most of the adsorption process it is expected that a greater portion of the chromatographic media come upon with a less concentrated solution for the long column (PG 700) as compared with the short column (PG 1000) for the same inlet superficial velocity and concentration. Hence, we have reached to better fits for the long column (PG 700) with D_s values of McCue et al. [10] corresponding to the lower range of 0.5–1.0 mg/mL initial tank concentration, whereas for PG 1000 better fits were obtained with D_s values corresponding to the upper range of 0.5–1.0 mg/mL initial tank concentration.

Local equilibrium assumption based PG 700 and PG 1000 packed column breakthrough profile simulations of McCue et al. [10], where the model equations were solved via orthogonal collocation on finite elements, are reproduced in Figs. 5 and 6, respectively (by permission from Elsevier). Comparison of the non-equilibrium simulations (Fig. 4) against local equilibrium based simulations (Figs. 5 and 6), where the same operation parameters are employed, clearly illustrates the superiority of the non-equilibrium model over local equilibrium assumption based pore diffusion and homogeneous surface diffusion models. McCue et al. [10] have repeated simulation studies both for pore and surface diffusion based local equilibrium models. These models fail in simulating the tails of experimental breakthrough profiles due to the assumption of instant equilibrium between bulk liquid and solid concentrations. Figs. 5 and 6 illustrates that local equilibrium assumption used by McCue et al. [10], as it does not take into account the mass transfer resistances, falsely predicts higher adsorption rates. On the other hand Fig. 4 shows that non-equilibrium model simulations of this study predicts lower adsorption rates that are in agreement with the experimental data of McCue et al. [10], i.e. the break point time of local equilibrium assumption based models becomes greater than that of the non-equilibrium predictions. The non-equilibrium model behaviors, presented in this study, indicate similar trends with the analysis of Harwell et al. [17]. Furthermore, if the local equilibrium assumption is used, breakthrough curves become steeper than that of non-equilibrium breakthrough curves, and initial "tailing" of the breakthrough

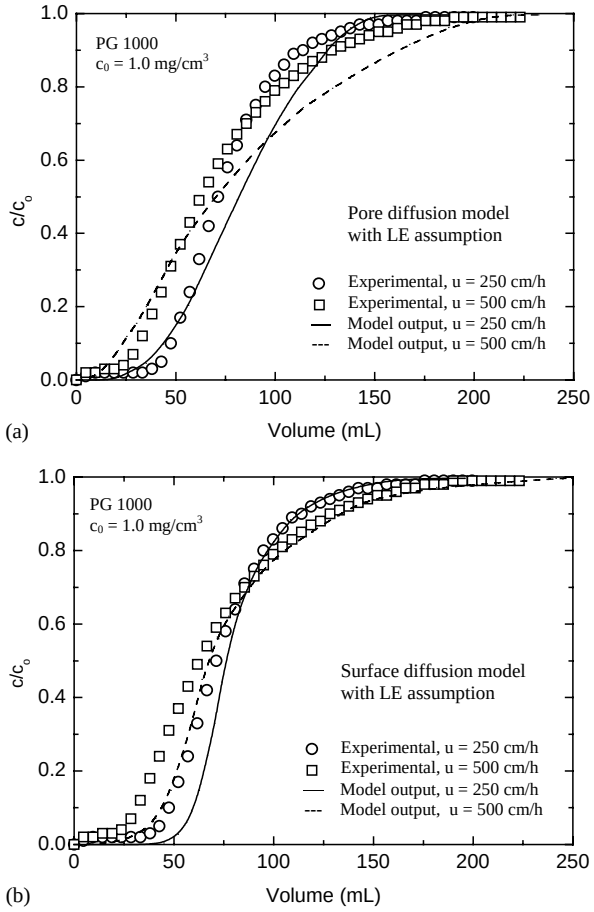

Fig. 6. Experimental and (a) pore diffusion, (b) homogeneous surface diffusion model (LE assumption) predicted breakthrough profiles of *h*IgG on PG 1000 chromatography media. *Note*: Experimental data of Fig. 5 of McCue et al. [10] are kindly supplied by the authors, with permission from Elsevier, Copyright (2003).

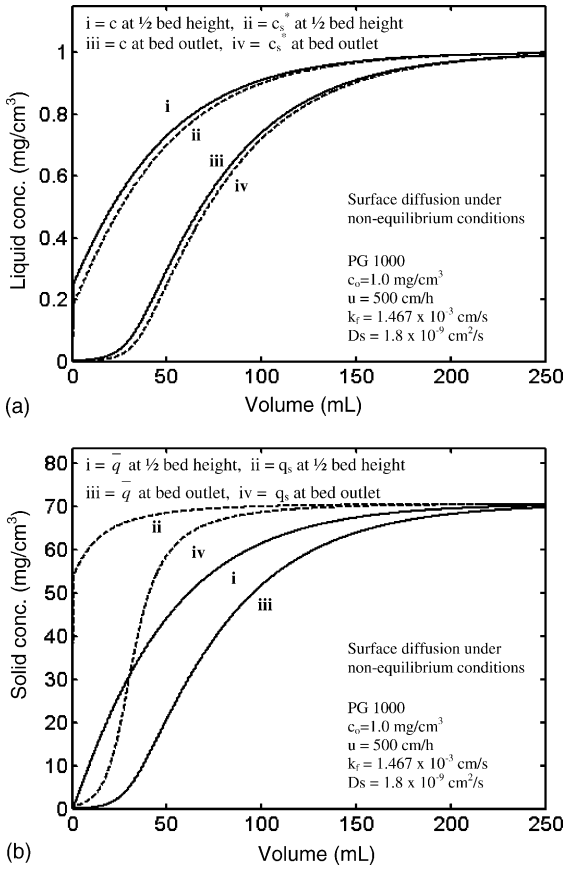

Fig. 7. Non-equilibrium model predicted PG 1000 chromatography media packed-bed chromatographic column for high feed inlet concentration: (a) interphase and bulk liquid concentration patterns, (b) solid surface and solid average concentration patterns. Operating parameters are the same with that of Fig. 4a.

curve disappear. Thus, the assumption of local equilibrium incorrectly predicts a narrower mass transfer zone than actually is present. McCue et al. [10] have based their orthogonal collocation numerical solution methodology on a "coupled" partial differential equation (PDE) system with two sets of mass balance equations in the bulk fluid and particle phases. In the present approach, we used a simpler procedure that obviates the solution of "coupled" PDE systems. The numerical solution strategy of this work is based on the implicit scheme finite differences technique for the solution of a single PDE by taking the advantage that, to a good approximation at a specified bed location, the difference between "one time step prior to the present time particle phase concentration" and "the present time particle phase concentration" is negligible for a small increment in time.

With the aid of the non-equilibrium model, the correlations between: (a) interphase and bulk liquid concentrations; (b) solid surface and solid average concentrations for PG 1000 chromatography media packed chromatographic column are presented in Fig. 7. The correlations using the same parameters with that of Fig. 4a is presented at Fig. 7, which illustrates that, the difference between interphase and bulk liquid concentrations are small, but there is a substantial difference between solid surface and solid average concentrations due to the relatively small D_s value, ie. large internal resistance.

In order observe the influence of the feed concentration model simulation is repeated using the parameter values of Fig. 7 but the value of c_0 is decreased by a factor of 10. Fig. 8 illustrates non-equilibrium model simulations at feed concentration of 0.1 mg/cm^3. Fig. 8 shows that at the total bed height outlet, due to the low solute concentration of the feed, the values of c, c_s^* and $\bar{q}$, q_s start to appear only at the end of the simulation period. However, the comparison of Figs. 7 and 8 for 1/2 bed height reveals that at the low feed inlet concentration (Fig. 8a) the percent difference between c and c_s^* increases as compared with that of high feed inlet concentration (Fig. 7a). This might be attributed to the predomination of film resistance at low solute concentration. Furthermore, for high feed inlet concentration the difference between solid surface concentration q_s and solid average concentration $\bar{q}$ becomes notable, whereas for low feed inlet concentration the difference between q_s and $\bar{q}$ becomes less significant, as shown in Figs. 7b and 8b, respectively. This indicates that the solid phase resistance might become the critical step for high feed inlet concentrations.

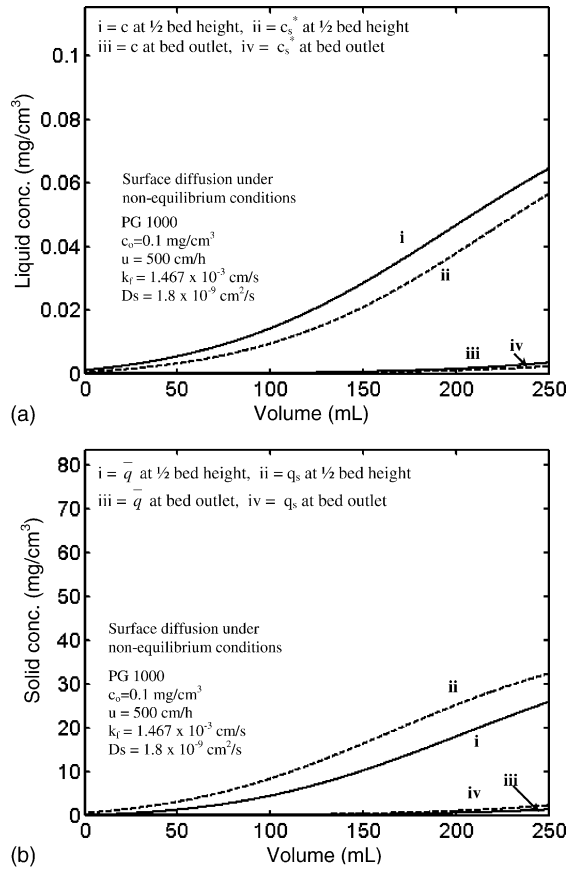

Fig. 8. Non-equilibrium model predicted PG 1000 chromatography media packed-bed chromatographic column for low feed inlet concentration: (a) interphase and bulk liquid concentration patterns, (b) solid surface and solid average concentration patterns. Operating parameters are the same with that of Fig. 4a with the exception that the value of c_0 is decreased by a factor of 10.

4. Conclusion

In this work a new mathematical model, based on non-equilibrium conditions, describing the dynamic adsorption of proteins in columns packed with spherical adsorbent particles is used to study the performance of chromatographic systems. The method commences with a general model, where combination of external mass transfer and intra-particle transport by solid (surface) diffusion is employed. The present analysis showed that the oversimplification of packed-bed adsorption with models based on assumptions of local equilibrium, leads to the erroneous predictions of breakthrough curves. Comparison of the non-equilibrium model predicted bulk liquid concentration and the corresponding interphase liquid concentration illustrate that there are substantial differences between them. This is especially true for the early stages of adsorbent loading. Furthermore, it was concluded that the local equilibrium assumption falsely implies a narrower mass transfer zone than actually it is. A local equilibrium assumption should thus be made only for qualitative estimates of break point times for real systems. The present study illustrates that; there is a noticeable difference between adsorbent particle surface concentration and its average concentration. The adsorbent loading status and thus the time, seriously alter the difference between adsorbent particle surface concentration and its average concentration.

5. Nomenclature

Bi	Biot number ($k_f r_p / D_s$)
c	liquid concentration in the void fraction of packed-bed adsorption column (mg/cm^3)
c_0	liquid concentration at the packed-bed inlet (mg/cm^3)
c_i^*	interphase liquid concentration (mg/cm^3)
D	free diffusivity of *h*IgG in water (cm^2/s)
D_a	axial dispersion coefficient (cm^2/s)
D_s	surface (solid) diffusivity (cm^2/s)
h	increment in distance (cm)
i	x panel index used in numerical solution
j	t panel index used in numerical solution
k	increment in time (s)
k_f	film mass transfer coefficient (cm/s)
K_L	constant in Langmuir isotherm (cm^3/mg)
L	packed-bed height (cm)
Pe	Peclet number based on interstitial fluid velocity ($2r_p v / D_a$)
$\bar{q}$	adsorbent particle average concentration (mg/cm^3 solid)
q_m	Langmuir isotherm maximum adsorption capacity (mg/cm^3 solid)
q_s	solid concentration at the adsorbent surface (mg/cm^3 solid)
r	radial coordinate (cm)
r_p	adsorbent particle average radius (cm)
R_c	column inside radius (cm)
Re	Reynolds number based on superficial fluid velocity ($2r_p u \rho / \mu$)
Sc	Schmidt number ($\mu / \rho D$)
Sh	Sherwood number ($2r_p k_f / D$)
t	time (s)
u	superficial velocity (cm/s)
v	interstitial velocity (cm/s)
x	packed-bed axial distance (cm)

Greek letters

α	parameter equal to $kv/(2h)$
β	parameter equal to $3(1-\varepsilon)k_f/(\varepsilon r_p)$
ε	void fraction in packed-bed adsorber
γ	parameter equal to kD_a/h^2
μ	liquid phase viscosity (kg/m s)
ρ	liquid phase density (kg/m^3)

References

[1] A.P. Coppola, M.D. Levan, Chem. Eng. Sci. 38 (1983) 991.
[2] J.A. Ritter, R.T. Yang, Chem. Eng. Sci. 46 (1991) 563.
[3] G. Carta, A. Cincotti, Chem. Eng. Sci. 53 (1998) 3483.
[4] G.A. Heeter, A.I. Liapis, J. Chromatogr. A 796 (1998) 157.
[5] H. Kempe, A. Axelsson, B. Nilsson, G. Zacchi, J. Chromatogr. A 846 (1999) 1.
[6] S.W. Rutherford, D.D. Do, Carbon 38 (2000) 1339.
[7] J. Mugge, H. Bosch, T. Reith, Chem. Eng. Sci. 56 (2001) 5351.
[8] J.M. Chern, Y.W. Chien, Water Res. 36 (2002) 647.
[9] D.D. Frey, C.R. Narahari, C.D. Butler, AIChE J. 48 (2002) 561.
[10] J.T. McCue, G. Kemp, D. Low, I. Quinones-Garcia, J. Chromatogr. A 989 (2003) 139.
[11] J.M. Schork, J.R. Fair, Ind. Eng. Chem. Res. 27 (1998) 457.
[12] C.K. Lee, Q. Yu, S.U. Kim, N.-H.L. Wang, J. Chromatogr. 484 (1989) 29.
[13] Q.M. Mao, A. Johnston, I.G. Prince, M.T.W. Hearn, J. Chromatogr. 548 (1991) 147.
[14] C. Yao, C. Tien, Chem. Eng. Sci. 47 (1992) 457.
[15] C. Yao, C. Tien, Chem. Eng. Sci. 47 (1992) 465.
[16] I. Zwiebel, C.M. Kralik, J.J. Schnitzer, AIChE J. 20 (1974) 915.
[17] J.H. Harwell, A.I. Liapis, R. Litchfield, D.T. Hanson, Chem. Eng. Sci. 35 (1980) 3483.
[18] E. Santacesaria, M. Morbidelli, A. Servida, G. Storti, S. Carra, Ind. Eng. Chem. Process Des. Dev. 21 (1982) 446.
[19] H. Moon, W.K. Lee, Chem. Eng. Sci. 41 (1986) 1995.
[20] G.L. Skidmore, B.J. Hortsmann, H.A. Chase, J. Chromatogr. 498 (1990) 113.
[21] J.H. Yun, D.K. Choi, H. Moon, Chem. Eng. Sci. 55 (2000) 5857.
[22] M.V. Ernest, R.D. Whitley Jr., Z. Ma, N.-H.L. Wang, Ind. Eng. Chem. Res. 36 (1997) 212.
[23] G.M. Zhong, F. Meunier, Chem. Eng. Sci. 48 (1993) 1309.
[24] G.M. Zhong, F. Meunier, Chem. Eng. Sci. 48 (1993) 4105.
[25] T. Vermeulen, in: T.B. Drew, J.W. Hoopes Jr. (Eds.), Advances in Chemical Engineering, vol. 2, Academic Press, New York, 1958, p. 147.
[26] U.K. Traegner, M.T. Suidan, B.R. Kim, Water Res. 30 (1996) 1495.
[27] G. McKay, M. El-Geundi, M.M. Nassar, Trans. IChemE (Part B) 74 (1996) 277.
[28] K.K.H. Choy, J.F. Porter, G. McKay, Chem. Eng. Sci. 59 (2004) 501.
[29] W.J. Weber, K.T. Liu, Chem. Eng. Commun. 6 (1980) 49.
[30] D. Chatzopoulos, A. Varma, Chem. Eng. Sci. 50 (1995) 127.
[31] E.H. Smith, Chem. Eng. Commun. 159 (1997) 17.
[32] G. McKay, Chem. Eng. J. 81 (2001) 213.
[33] I. Prasetyo, H.D. Do, D.D. Do, Chem. Eng. Sci. 57 (2002) 133.
[34] A.I. Liapis, D.W.T. Rippin, Chem. Eng. Sci. 33 (1978) 593.
[35] K. Kaczmarski, M. Mazzotti, G. Storti, M. Morbidelli, Comput. Chem. Eng. 21 (1997) 641.
[36] G. Xiu, P. Li, A.E. Rodrigues, Chem. Eng. J. 95 (2003) 83.
[37] E. Glueckauf, J.I. Coates, J. Chem. Soc. (1947) 1315.
[38] M. Goto, J.M. Smith, B.J. McCoy, Chem. Eng. Sci. 45 (1990) 443.
[39] A. Tejeda-Mansir, R.M. Montesinos, R. Guzman, J. Biochem. Biophys. Methods 49 (2001) 1.
[40] I. Langmuir, J. Am. Chem. Soc. 38 (1916) 2221.
[41] I. Quinones, C.M. Grill, L. Miller, G. Guiochon, J. Chromatogr. A 867 (2000) 1.
[42] G. Linfield, J. Penny, Numerical Methods Using Matlab, Ellis Horwood, New York, 1995.
[43] A.R. Özdural, D. Tanyolaç, Z. Demircan, I.H. Boyaci, M. Mutlu, C. Webb, Chem. Eng. Sci. 56 (2001) 3483.
[44] A.R. Özdural, D. Tanyolaç, I.H. Boyaci, M. Mutlu, C. Webb, Biochem. Eng. J. 14 (2003) 27.
[45] A.R. Özdural, A. Alkan, J. Memb. Sci. 223 (2003) 49.
[46] J.T. McCue, Millipore corporation, Biopharmaceutical division, Bedford, MA 01730, USA, 2003, personal communication.
[47] E.J. Wilson, C.J. Geankoplis, Ind. Eng. Chem. Fundam. 5 (1966) 9.
[48] T.K. Sherwood, R.L. Pigford, C.R. Wilke, Mass Transfer, McGraw Hill, New York, 1975.
[49] J.M. Coulson, J.F. Richardson, Chemical Engineering, 4th ed., vol. 2, Pergamon Press, Oxford, 1991.
[50] S.F. Chung, C.Y. Wen, AIChE J. 14 (1968) 857.